Geophysical Research Letters

RESEARCH LETTER
10.1029/2020GL087250

Special Section:
Years of the Maritime Continent

MJO Propagation Across the Maritime Continent: Are CMIP6 Models Better Than CMIP5 Models?

Min-Seop Ahn[1,2], Daehyun Kim [1], Daehyun Kang[1], Jiwoo Lee[3], Kenneth R. Sperber[3], Peter J. Gleckler[3], Xianan Jiang[4,5], Yoo-Geun Ham [2], and Hyemi Kim[6]

[1]Department of Atmospheric Sciences, University of Washington, Seattle, WA, USA, [2]Department of Oceanography, Chonnam National University, Gwangju, South Korea, [3]PCMDI, Lawrence Livermore National Laboratory, Livermore, CA, USA, [4]Joint Institute for Regional Earth System Science and Engineering, University of California, Los Angeles, CA, USA, [5]Jet Propulsion Laboratory, California Institute of Technology, Pasadena, CA, USA, [6]School of Marine and Atmospheric Sciences, Stony Brook University, Stony Brook, NY, USA

Abstract Many climate models struggle with a poor simulation of the Madden-Julian Oscillation (MJO), especially its propagation across the Maritime Continent (MC). This study quantitatively evaluates the robustness of MJO propagation over the MC in climate models that participated in Coupled Model Intercomparison Project Phase 5 (CMIP5) and Phase 6 (CMIP6) with a newly developed MC propagation metric. The results show that the CMIP6 models simulate MJO propagation over the MC more realistically than the CMIP5 models. Lower free-tropospheric moisture budget analysis highlights that the greater horizontal moisture advection is responsible for the enhanced MJO propagation over the MC. The increase in horizontal moisture advection in the CMIP6 models is mainly attributed to the steeper horizontal mean state moisture gradient around the MC, which is associated with the reduction of the equatorial dry bias.

Plain Language Summary The Madden-Julian Oscillation (MJO), planetary-scale eastward propagating tropical convective cloud clusters coupled with large-scale circulation, is the dominant mode of intraseasonal variability in the tropics and thereby influences a wide range of weather and climate phenomena. Unfortunately, however, many contemporary climate models struggle to simulate a realistic MJO propagation across the Maritime Continent, and this common bias had persisted over the previous generations of the Coupled Model Intercomparison Project (CMIP). We show that, in the newly released CMIP Phase 6 (CMIP6) models, the simulation of the MJO propagation is significantly improved when compared to their predecessors—CMIP Phase 5 (CMIP5) models. The improvement in the MJO simulation is mainly due to the reduction of the dry bias that many CMIP5 models exhibit over the Indo-Pacific Warm Pool region.

Key Points:
- A metric indicating the robustness of MJO propagation across the MC is developed and applied to 30 CMIP5 and 34 CMIP6 models
- CMIP6 models represent MJO propagation over the MC more realistically than the CMIP5 models
- The improvement in MJO propagation is due to the steepening of the mean state moisture gradient around the MC

Supporting Information:
- Supporting Information S1

Correspondence to:
D. Kim and Y.-G. Ham,
daehyun@uw.edu;
ygham@jnu.ac.kr

Citation:
Ahn, M.-S., Kim, D., Kang, D., Lee, J., Sperber, K. R., Gleckler, P. J., et al. (2020). MJO propagation across the Maritime Continent: Are CMIP6 models better than CMIP5 models? *Geophysical Research Letters*, *47*, e2020GL087250. https://doi.org/10.1029/2020GL087250

Received 27 JAN 2020
Accepted 2 MAY 2020
Accepted article online 10 MAY 2020

©2020. The Authors.
This is an open access article under the terms of the Creative Commons Attribution License, which permits use, distribution and reproduction in any medium, provided the original work is properly cited.

1. Introduction

The Madden-Julian Oscillation (MJO, Madden & Julian, 1971, 1972) is a planetary-scale, eastward propagating envelop of tropical convection that is tightly coupled with large-scale circulation. The MJO influences a wide range of weather and climate phenomena not only in the tropics but also in the midlatitude and high-latitude regions by its teleconnections (see a review by Zhang, 2013). For example, when the MJO convection is located over the Western Pacific, the frequency of flood events increases over the Philippines and the West Coast of North America (Bond & Vecchi, 2003; Zhang, 2013), tropical cyclones occur more frequently over the Western Pacific (Klotzbach, 2014; Zhang, 2013), and more frequent westerly wind burst events occur in the Western Pacific that can trigger El Niño development (Hendon et al., 2007; Zhang, 2013).

The Indo-Pacific Maritime Continent (MC), the largest archipelago on Earth, resides between the Indian Ocean and the Western Pacific. This is an important region regarding the MJO's life cycle and its teleconnections. Because more than one half of all MJO events initiate over the Indian Ocean (Zhang & Ling, 2017), whether an MJO event successfully passes through the MC determines the longevity and zonal extent of the event. Also, MJO teleconnections to the extratropics have been shown to intensify while the MJO convection is propagating over the MC (Adames & Wallace, 2014; Bao & Hartmann, 2014). Therefore, for a climate model to accurately simulate the impacts of the MJO on the global weather-climate system, it must realistically represent MJO propagation across the MC.

Unfortunately, however, many contemporary climate models fail to simulate realistic MJO propagation across the MC (Ahn et al., 2017; Hung et al., 2013; Jiang et al., 2015; Kim et al., 2009; Lin et al., 2006; Ling et al., 2019) and this bias has been pervasive over recent generations of climate models participating in the Coupled Model Intercomparison Project (CMIP). Lin et al. (2006) and Hung et al. (2013) analyzed CMIP3 and CMIP5 models, respectively, using the same lag-regression diagnostic of precipitation anomalies to examine the MJO propagation. When considering propagation through 150°E longitude as a criterion of MJO fidelity over the MC in the lag-longitude diagram, only 4–5 out of 14 (28–36%) CMIP3 models show realistic MJO propagation across the MC (Lin et al., 2006), and only 4–7 out of 20 (20–35%) CMIP5 models satisfy this criterion (Hung et al., 2013). As the CMIP6 models are newly released, there is a critical need to analyze the CMIP6 models to examine whether they are better than the CMIP5 models in the simulation of the MJO propagation across the MC.

In support of community efforts to establish objective tests to gauge how well climate models represent various observed characteristics (e.g., Baker & Taylor, 2016; Flato et al., 2013; Gleckler et al., 2008; Gleckler et al., 2016; Lee et al., 2019), a diverse collection of community-based MJO simulation diagnostics and metrics has been developed to capture the prominent characteristics of the MJO (Kiladis et al., 2014; MJOWG, 2009; Sperber & Kim, 2012; Wheeler & Hendon, 2004; Wheeler & Kiladis, 1999; Zhang & Ling, 2017). However, to date, little attention has been given to quantifying the robustness of MJO propagation over a specific region. We propose a new metric that focuses on the MJO's behavior over the MC, which will then be utilized to quantitatively evaluate the CMIP5 and CMIP6 models.

As it will be shown that there is a robust improvement in the representation of MJO propagation over the MC in the CMIP6 models, another goal of the present study is to understand the difference between the two model generations (CMIP5 vs. CMIP6) in the context of the moisture mode framework. In the moisture mode framework, the propagation and maintenance of the MJO are understood by diagnosing the physical factors that give rise to the moisture anomalies (Adames et al., 2020; Adames & Kim, 2016; Fuchs & Raymond, 2017; Raymond & Fuchs, 2009; Sobel & Maloney, 2013). We will analyze the moisture budget of the MJO in CMIP5 and CMIP6 models to identify the processes responsible for the differences in MJO propagation between the two model groups.

2. Data and Methods

2.1. Models and Validation Data Set

Thirty CMIP5 (Taylor et al., 2012) and 34 CMIP6 (Eyring et al., 2016) models analyzed in this study are listed in Table S1 in the supporting information. We use one ensemble member of each model—r1i1p1 for all CMIP5 models and r1i1p1f1 for all CMIP6 models except for CNRM (r1i1p1f2), HadGEM3 (r1i1p1f3), MIROC-ES2L (r1i1p1f2), and UKESM1 (r1i1p1f2) models. Daily-averaged precipitation, specific humidity, and horizontal wind from the historical run for a common 20-year period (1985–2004) are obtained from the archive. As references for model simulations, we use four data sets of daily mean precipitation: the Tropical Rainfall Measuring Mission 3B42 Version 7 (TRMM, Huffman et al., 2007), the Climate Prediction Center morphing method (CMORPH, Joyce et al., 2004) for 20 years (1998–2017), and the fifth generation of the European Center for Medium-Range Weather Forecasts (ECMWF) Reanalysis (ERA5, Hersbach et al., 2019) for two 20-year periods (1985–2004 and 1998–2017). We use daily mean specific humidity and horizontal wind from ERA5 for 20 years (1998–2017). For specific humidity, we also use ERA5 for the period 1985–2004 to compare the mean state with the same period of model simulations. All participating models and validation data are interpolated into 2.5° longitude and 2.5° latitude horizontal resolution, and the analysis is performed for boreal winter (November–April) when the MJO is the most active.

2.2. MC Propagation Metric

We propose a new metric that is designed to indicate the robustness of MJO propagation over the MC. The metric, which will be called the "MC propagation metric," is obtained from one of the popular MJO simulation diagnostics: the lag-regression diagnostic. To yield a diagram that shows the behaviors of anomalous convection before and after it peaks over the Indian Ocean, 10°S to 10°N averaged intraseasonal (i.e., 20–100-days band-pass filtered) precipitation anomalies are regressed against a reference Indian Ocean (85–95°E and 5°S to 5°N) intraseasonal precipitation time series and the results are plotted in a lag-longitude

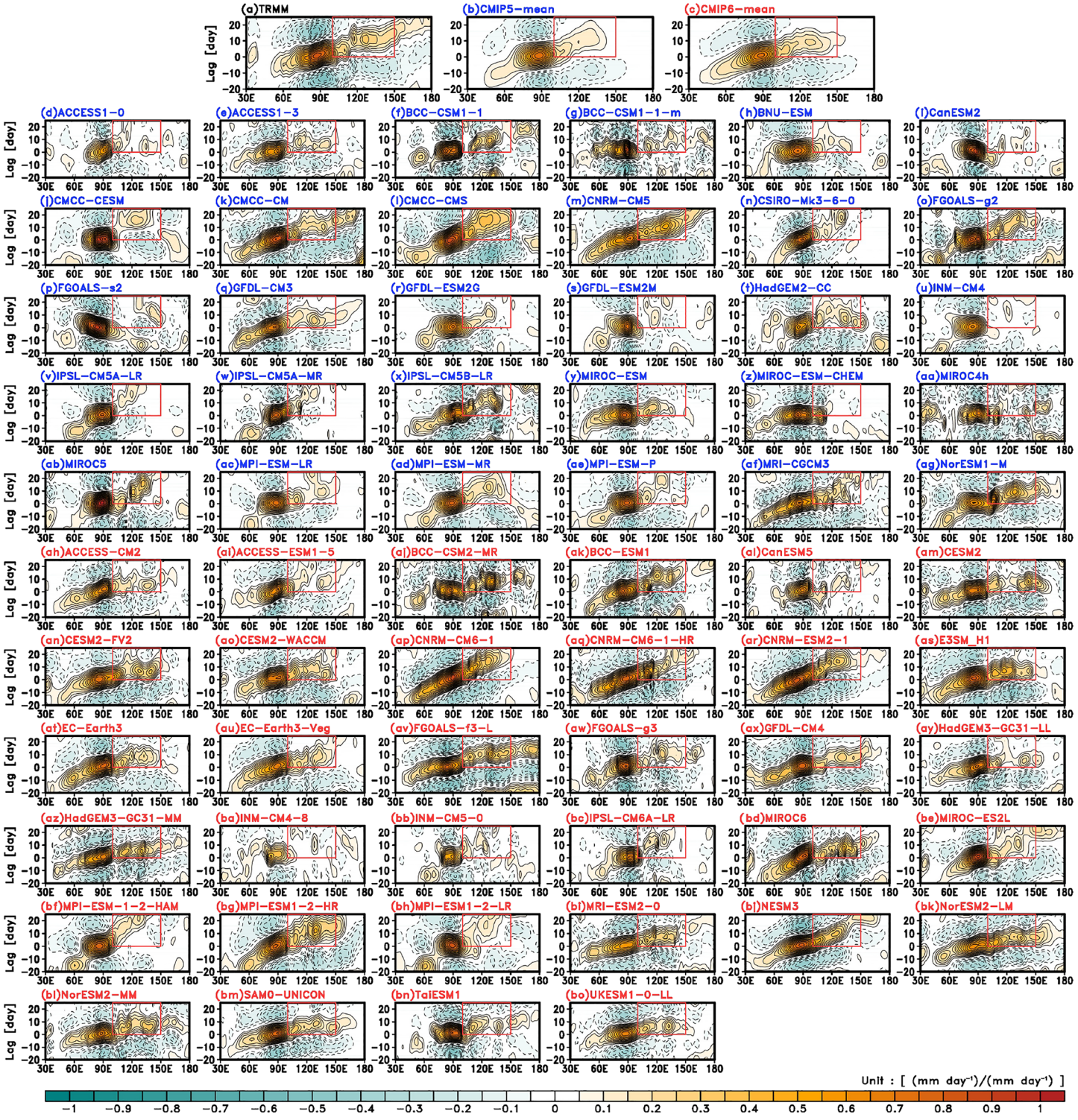

Figure 1. Lag-longitude diagram of precipitation for (a) TRMM, (b) 30 CMIP5 mean, (c) 34 CMIP6 mean, and (d—bo) each individual model. The lag-longitude diagram is obtained as lag-regression of 10°S to 10°N averaged 20- to 100-day band-pass-filtered precipitation anomalies against its time series averaged over the 85–95°E and 5°S to 5°N. The blue and red colors on the model names indicate CMIP5 and CMIP6, respectively. The red box in each panel indicates the area and lag days that are used for the MC propagation metric.

diagram (Figure 1). From the lag-longitude diagram, the positive regression coefficients over the MC area (100–150°E) and over 0–25 lag days are summed. The sum is then normalized by the TRMM observed value to yield the MC propagation metric (Figure 2).

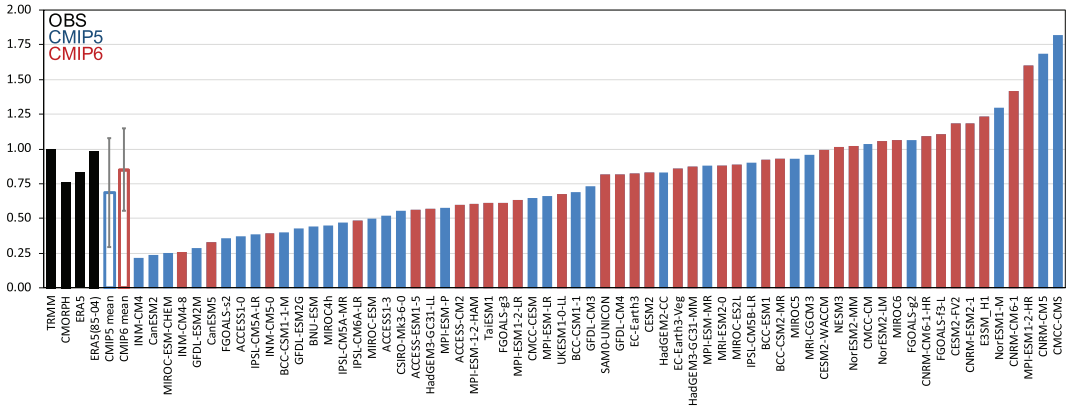

Figure 2. Bar graph of MC propagation metric for TRMM, CMORPH, ERA5 of 1998–2017, ERA5 of 1985–2004, 30 CMIP5 mean, 34 CMIP6 mean, and each individual model with an ascending order. The MC propagation metric is obtained as a sum of positive regression coefficients over the MC area (100–150°E and 0–25 lag days) in the lag-longitude diagram shown in Figure 1 normalized by the TRMM observed value. The vertical lines on the multimodel means indicate the intermodel spread of the model group obtained as one standard deviation.

2.3. Moisture Budget Analysis

The moisture budget of the MJO is analyzed to understand the moisture evolution associated with the MJO. Two vertical levels in the low free troposphere—850 and 700 hPa—are used. The low free-tropospheric moisture is tightly coupled to MJO convection in the intraseasonal time scales and the MJO-associated moisture anomaly peaks around 700 hPa (Adames & Wallace, 2015; Kiladis et al., 2005; Sperber, 2003). The low free-tropospheric moisture equation for MJO anomalies is written as follows:

$$\frac{\partial q'}{\partial t} = -u\frac{\partial q'}{\partial x} - v\frac{\partial q'}{\partial y} - \omega\frac{\partial q'}{\partial p} - C' + E'$$

where q, u, v, and ω are the specific humidity, zonal velocity, meridional velocity, and vertical pressure velocity, respectively. C and E are the condensation and evaporation. The angled bracket indicates a mass weighed integral from 850 to 700 hPa, and the prime indicates MJO anomalies. The MJO anomalies are obtained from the lag-regression analysis of each intraseasonal moisture budget term against the same Indian Ocean reference time series that is used for the lag-regression diagnostic in Figure 1. The tendency, zonal and meridional advection terms are calculated using available model output variables, and the sum of the other terms is obtained as a residual.

3. Results

Figure 1 shows the lag-longitude diagrams for TRMM, and for 30 CMIP5 and 34 CMIP6 models. Also shown in Figure 1 are the multimodel mean of the diagrams for the two model groups (Figures 1b and 1c). In the TRMM observations the MJO's eastward propagation is clearly seen from the Indian Ocean to the Western Pacific with a propagation speed of about 5 m/s. Over the MC region and for the positive lag days, the regression coefficients are greater than 0.2 in many longitude points over several days.

While some CMIP5 models are capable of representing the observed eastward propagation of the MJO over the MC region (e.g., CMCC-CM, CMCC-CMS, CNRM-CM5, FGOALS-g2, MRI-CGCM3, and NorESM1-M), many CMIP5 models fail to exhibit an MJO signal over the MC (Figures 1d–1ag), a conclusion that is consistent with that from previous assessments (Ahn et al., 2017; Hung et al., 2013). On the contrary, in many CMIP6 models, there is a clear indication of eastward propagation in the MC region, except for some models (e.g., ACCESS-ESM 1-5, CanESM5, HadGEM3-GC3-LL, INM-CM4-8, INM-CM5-0, and IPSL-CM6A-LR).

When averaged over the two model groups, the CMIP5 multimodel mean shows weaker eastward propagation over the MC region in the positive lag days, with the regression coefficients showing values near 0.1. The lag-longitude diagram for the CMIP6 multimodel mean is much closer to the observations in its pattern and

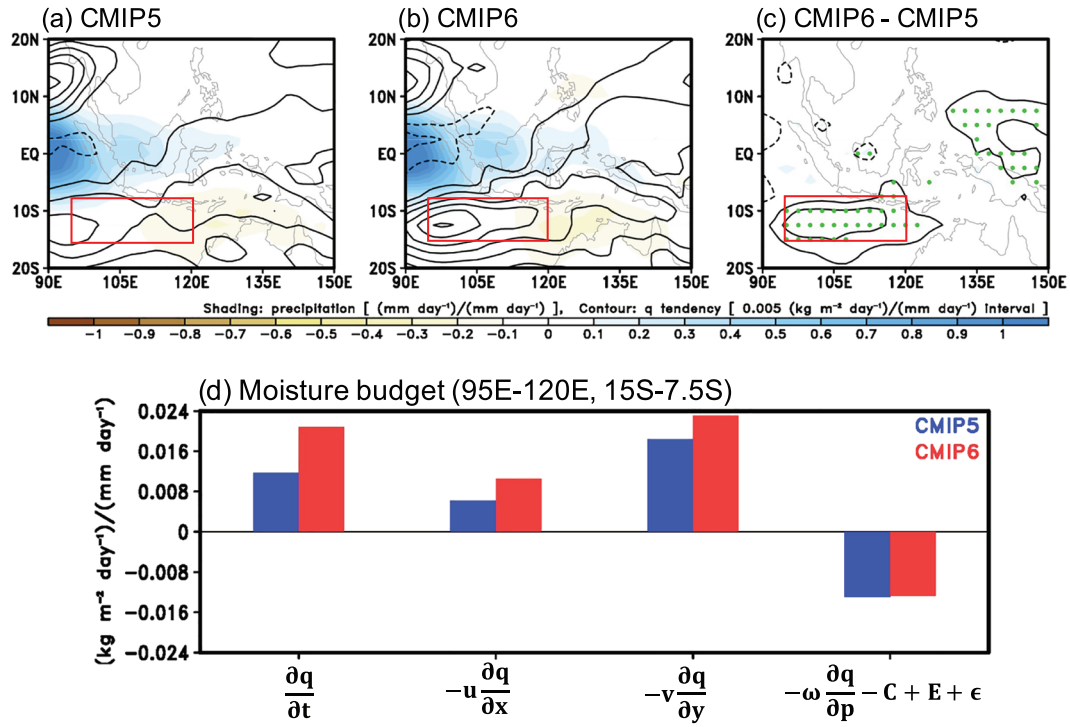

Figure 3. (a–c) Regressed horizontal patterns of precipitation (shading) and 850–700 hPa integrated q tendency (contour) anomalies for (a) 30 CMIP5 mean, (b) 34 CMIP6 mean, and (c) their difference. (d) Regressed 850–700 hPa integrated q budget averaged over the 95–120°E and 15–7.5°S. The regressed pattern of each variable is obtained as lagged regression of 20–100 days filtered variable against 20- to 100-day filtered precipitation time series averaged over the 85–95°E and 5°S to 5°N and averaged during lag −1 to +1 day. Green dots in the difference pattern indicate statistical significance at the 95% confidence level.

magnitude, clearly indicating that there is an improvement from the CMIP5 to the CMIP6 models in the representation of MJO propagation over the MC.

Figure 2 shows the MC propagation metric for observations, CMIP5 mean, CMIP6 mean, as well as individual CMIP5 and CMIP6 models in ascending order. The MC propagation metric reasonably distinguishes models with robust MJO propagation over the MC from those that poorly simulate it. For example, the models with a relatively large value of the metric (e.g., CMCC-CMS, CNRM-CM5, and MPI-ESM 1-2-HR) show pronounced MJO-associated precipitation anomalies over the MC in the lag-longitude diagram (Figure 1), whereas the models with a relatively small value (e.g., INM-CM4, CanESM2, and MIROC-ESM-CHEM) do not exhibit MJO eastward propagation over the MC. In the CMIP5 ensemble, the MC propagation metric is severely underestimated—less than half of the observed value (<0.5)—for about 43% of all models (13 out of 30). On contrary, only about 12% (4 out of 34) CMIP6 models show MC propagation metric lower than 0.5. The relatively good models with the metric value between 0.75 and 1.25 are only about 23% (7 out of 30) for CMIP5 models but about 59% (20 out of 34) for CMIP6 models. Note that the period of TRMM data used here (1998–2017) is different from that of model data (1985–2004) due to data availability. To estimate the observational uncertainty, we show values obtained from ERA5 for 1985–2004 and 1998–2017, and CMORPH for 1998–2017. The results show that the four estimates of the MC propagation metric are not much different—the standard deviation of the four values is 0.103.

The multimodel mean values of the MC propagation metric show significant improvement in the CMIP6 models over the CMIP5 models. The multimodel mean value of the CMIP6 models is 0.85, while that of the CMIP5 models is 0.69. The difference between the two mean values is statistically significant at the 90% confidence level, but not at the 95% confidence level (p value ~0.06). Also, the intermodel spread is reduced by about 23% in CMIP6 (0.30) compared to CMIP5 (0.39) although the number of CMIP6 ensemble is larger. These results indicate that the representation of MJO propagation is notably improved over the MC area in the CMIP6 models compared to the CMIP5 models.

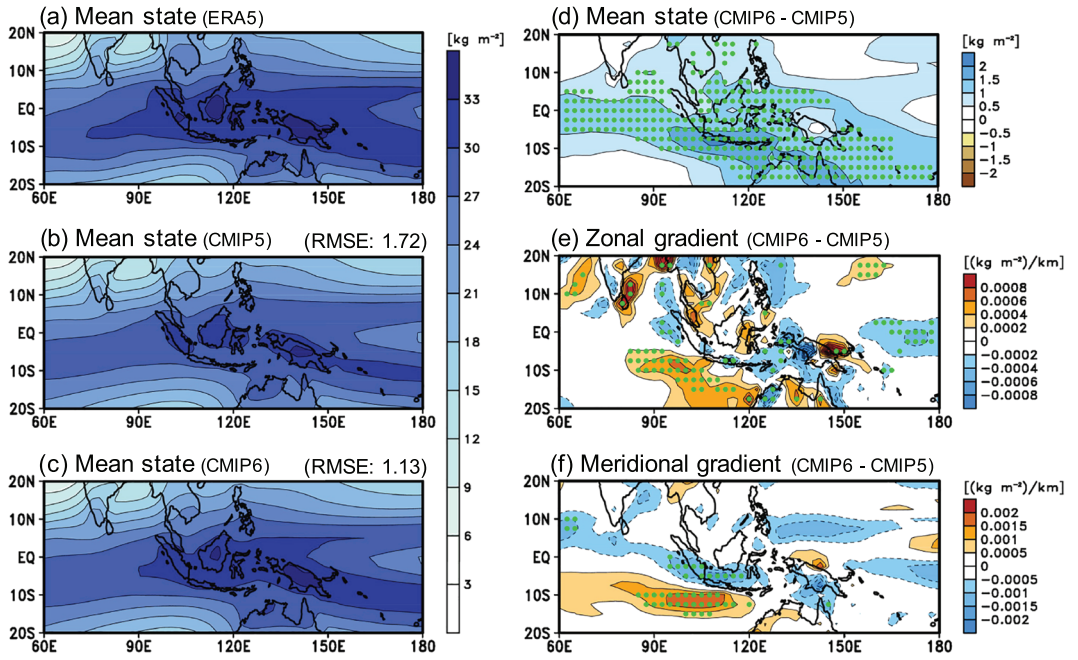

Figure 4. (a–c) The 850–700 hPa integrated q mean state patterns (November–April) for (a) ERA5 of 1985–2004, (b) 30 CMIP5 mean, and (c) 34 CMIP6 mean. The difference between CMIP5 mean and CMIP6 mean in (d) mean state, (e) zonal gradient of the mean state, and (f) meridional gradient of the mean state. Green dots in the difference patterns indicate the statistical significance at the 95% confidence level. The RMSE shown in the upper right corner of panels (b) and (c) is obtained against the observed mean state over the figure domain.

The low free-tropospheric moisture budget analysis is performed as described in section 2.3 to understand the improved simulation of MJO propagation in CMIP6 models from a moisture mode framework point of view. Figures 3a and 3b show intraseasonal precipitation (shading) and low free-tropospheric moisture tendency (contours) anomalies that are associated with MJO. When the center of enhanced MJO convection is located over the eastern Indian Ocean, positive low free-tropospheric moisture tendencies (solid contours) appear over the southern MC and the Western Pacific in both model generations. However, the moisture tendency to the south of Sumatra and Java Islands is much greater in the CMIP6 models than in the CMIP5 models. The difference between the two model groups in that area is statistically significant at the 95% confidence level (Figure 3c). The greater amount of moisture recharging over the southern MC area would provide a favorable condition for MJO propagation over the MC region in the CMIP6 models.

In Figure 3d, we compare the moisture budget terms over the southern MC area (95–120°E and 15–7.5°S, red box in Figures 3a–3c) between the two model groups. In the CMIP6 models, the total moisture tendency is about 2 times larger than that in the CMIP5 models, consistent with the above results. The zonal and meridional advection terms show positive values, indicating that horizontal moisture advection is the main recharging mechanism in this region before the onset of MJO convection. They also exhibit a larger value in the CMIP6 models, suggesting that the horizontal advection process is responsible for the difference in total moisture tendency. The sum of other terms and residual (right most bars in Figure 3d) is similar in the two model groups; thus, it is unable to explain the difference in the total moisture tendency. The results of the moisture budget analysis strongly suggest that MJO propagation in the MC area is more realistic in the CMIP6 models due to the greater rate of moisture recharging from the zonal and meridional advection processes.

Figure S1 shows that in both model groups the horizontal advection is mainly determined by the advection of mean state moisture by MJO perturbation wind, which is consistent with previous studies (e.g., Ahn et al., 2020; Kim et al., 2017; Jiang, 2017; Kim et al., 2014; Kim, 2017; Kiranmayi & Maloney, 2011). This suggests that the difference in the horizontal advection terms between the CMIP5 mean and the CMIP6 mean is likely due to the difference in the mean state moisture gradient. We show in Figures 4a–4c the low free-tropospheric mean state moisture from ERA5 and from the simulations. Compared to ERA5, the

CMIP5 multimodel mean exhibits a notable dry bias over the Indo-Pacific Warm Pool region, especially near the equator. The dry bias in the CMIP5 models has been reported in previous studies (e.g., Takahashi, 2018). The dry bias is remarkably improved in the CMIP6 multimodel mean. The root-mean-square error (RMSE) of the mean state moisture over the Indo-Pacific area (60–180°E and 20°S to 20°N) is also about 34% lower in CMIP6 (1.13) than in CMIP5 (1.72). The mean moisture difference between CMIP5 and CMIP6 models is statistically significant at the 95% confidence level over most of the Indo-Pacific Warm Pool region (Figure 4d).

The increase in the mean state moisture has direct implications for the gradient of the mean state moisture; a dry bias peaking near the equatorial MC would weaken the horizontal gradient, while removing the bias would steepen it. Figure 4e shows the difference in the zonal moisture gradient between the two model groups. The differences that are statistically significant are located south of Sumatra and Java Islands, with the gradient being larger in the CMIP6 models. The southern MC is the area where the rate of moisture recharging before the onset of MJO convection is greater in the CMIP6 models. The difference in the meridional moisture gradient (Figure 4f) is also statistically significant over the southern MC area. With the steeper mean state moisture gradient, all other conditions being equal, the same MJO wind anomaly would result in a greater moistening in the CMIP6 models than in the CMIP5 models. The results of our mean state analysis, when considered with the moisture budget analysis above, strongly suggests that the reduction of the dry bias in the MC region in the CMIP6 models helps them to better represent MJO propagation more realistically compared to the CMIP5 models.

4. Summary and Discussion

Many climate models share a common bias that the simulated MJO terminates over the MC too often, and this bias has persisted over the previous generations of CMIP models (Hung et al., 2013; Lin et al., 2006). In the current study, we developed a metric that indicates the robustness of MJO propagation over the MC and we applied it to 30 CMIP5 and 34 CMIP6 models to quantitatively evaluate whether the CMIP6 models are better than the CMIP5 models in simulating MJO propagation over the MC.

Our results showed that the MJO propagation skill over the MC is significantly improved in CMIP6 models compared to CMIP5 models. Using the MC propagation metric, 20 out of 34 (59%) CMIP6 models have values close to that observed (0.75–1.25), while only 7 out of 30 (23%) CMIP5 models exhibit such fidelity. In terms of the multimodel mean value of the MC propagation metric, the CMIP5 mean is about 69% of the observed value, whereas for CMIP6 it is about 85% of the observed value. This CMIP6 improvement is statistically significant at the 90% confidence level, but not at the 95% confidence level with a p value of about 0.06. Tables S2 and S3 compare the MC propagation index between two generations—CMIP5 and CMIP6—of models from the same institute. In 15 out of 16 model pairs, CMIP6 models show improvement (i.e., becomes closer to 1) over their CMIP5 versions. Although the CMIP6 models show robust improvement in the simulation of MJO propagation across the MC, many models still underestimate the observed metric.

Our process diagnosis indicates that the improvement in the MC propagation metric is related to the better representation of the mean state moisture around the MC. Probing deeper, the moisture budget analysis revealed that the improved MJO propagation over the MC in the CMIP6 mean is mainly attributed to the larger zonal and meridional moisture advection over the southern MC. The larger zonal and meridional moisture advection in CMIP6 mean are associated with the steepened horizontal gradient of mean state moisture over the southern MC. A dry bias over the Indo-Pacific Warm Pool region, which is pronounced in the CMIP5 models, almost disappears in the CMIP6 models, steepening the horizontal gradient of the mean state moisture over the southern MC area.

Our conclusion that the better MJO simulation in CMIP6 models is mainly due to the reduction of the dry bias is supported by the recent model intercomparison studies conducted by Gonzalez and Jiang (2017) and Jiang (2017). They also showed a systematic difference in the mean state moisture between relatively good- and poor-MJO models using climate models participating in the MJOTF/GASS MJO model intercomparison project. They showed that the models with robust MJO propagation tended to exhibit a wetter mean state over the tropics with a steeper horizontal moisture gradient over the MC area.

While this study highlights the role of the basic state moisture in the simulation of the MJO, our understanding of the processes that control the mean state moisture around the MC is still limited. Jiang et al. (2019) suggested that the MC diurnal cycle and topography play an important role on the formation of the mean state moisture around the MC. The improvement in the mean state moisture around MC in CMIP6 models is possibly due to the increased horizontal resolution, thus a better representation of MC island effects. Ahn et al. (2020) suggested that the intensity and convective top height of the MC land convection could modulate the mean state moisture around the MC with idealized model experiments in which the MC land convection is controlled to be shallower or deeper. More work is needed to better understand the processes that modulate the mean state moisture around the MC in a wide range of weather and climate systems.

Disclaimer

This document was prepared as an account of work sponsored by an agency of the U.S. government. Neither the U.S. government nor Lawrence Livermore National Security, LLC, nor any of their employees makes any warranty, expressed or implied, or assumes any legal liability or responsibility for the accuracy, completeness, or usefulness of any information, apparatus, product, or process disclosed, or represents that its use would not infringe privately owned rights. Reference herein to any specific commercial product, process, or service by trade name, trademark, manufacturer, or otherwise does not necessarily constitute or imply its endorsement, recommendation, or favoring by the U.S. government or Lawrence Livermore National Security, LLC. The views and opinions of authors expressed herein do not necessarily state or reflect those of the U.S. government or Lawrence Livermore National Security, LLC, and shall not be used for advertising or product endorsement purposes.

Acknowledgments

Constructive and valuable comments from the reviewers are greatly appreciated. M.-S. A., D. Kim, and D. Kang were supported by the NOAA CVP program (NA18OAR4310300), the U.S. DOE RGMA program (DE-SC0016223), and the NASA MAP program (80NSSC17K0227). D. Kim, H. K., and Y.-G. H. were also supported by KMA R&D program (KMI2018-03110). J. L., K. S., and P. G.'s work was performed under the auspices of the U. S. DOE (BER, RGMA Program) by LLNL under Contract DE-AC52-07NA27344. X. J. acknowledges support by the NOAA Climate Program Office under awards NA17OAR4310261. We thank DOE's RGMA program area, the Data Management program, and NERSC for making this coordinated CMIP6 analysis activity possible. For CMIP, the U.S. DOE's PCMDI provides coordinating support and led development of the software infrastructure in partnership with the Global Organization for Earth System Science Portals. The ESGF provided the CMIP model data (https://esgf-node.llnl.gov/projects/esgf-llnl). The TRMM provided the precipitation data (https://pmm.nasa.gov/data-access/downloads/trmm). The CMORPH provided the precipitation data (https://www.cpc.ncep.noaa.gov/products/janowiak/cmorph_description.html). The ECMWF provided the fifth generation of ECMWF reanalysis (ERA5, https://www.ecmwf.int/en/forecasts/datasets/reanalysis-datasets/era5).

References

Adames, Á. F., & Kim, D. (2016). The MJO as a dispersive, convectively coupled moisture wave: Theory and observations. *Journal of the Atmospheric Sciences*, *73*(3), 913–941. https://doi.org/10.1175/JAS-D-15-0170.1

Adames, Á. F., Kim, D., Maloney, E. D., & Sobel, A. H. (2020). The moisture mode framework of the Madden-Julian Oscillation. Chap. 22 in The multiscale global monsoon system, Vol. 11. https://doi.org/10.1016/j.ibmb.2020.103368

Adames, Á. F., & Wallace, J. M. (2014). Three-dimensional structure and evolution of the MJO and its relation to the mean flow. *Journal of the Atmospheric Sciences*, *71*(6), 2007–2026. https://doi.org/10.1175/JAS-D-13-0254.1

Adames, Á. F., & Wallace, J. M. (2015). Three-dimensional structure and evolution of the moisture field in the MJO. *Journal of the Atmospheric Sciences*, *72*(10), 3733–3754. https://doi.org/10.1175/JAS-D-15-0003.1

Ahn, M.-S., Kim, D., Ham, Y.-G., & Park, S. (2020). Role of maritime continent land convection on the mean state and MJO propagation. *Journal of Climate*, *33*(5), 1659–1675. https://doi.org/10.1175/JCLI-D-19-0342.1

Ahn, M.-S., Kim, D., Sperber, K. R., Kang, I.-S., Maloney, E., Waliser, D., & Hendon, H. (2017). MJO simulation in CMIP5 climate models: MJO skill metrics and process-oriented diagnosis. *Climate Dynamics*, *49*(11–12), 4023–4045. https://doi.org/10.1007/s00382-017-3558-4

Baker, N. C., & Taylor, P. C. (2016). A framework for evaluating climate model performance metrics. *Journal of Climate*, *29*(5), 1773–1782. https://doi.org/10.1175/JCLI-D-15-0114.1

Bao, M., & Hartmann, D. L. (2014). The response to MJO-like forcing in a nonlinear shallow-water model. *Geophysical Research Letters*, *41*, 1322–1328. https://doi.org/10.1002/2013GL057683

Bond, N. A., & Vecchi, G. A. (2003). The influence of the Madden–Julian Oscillation on precipitation in Oregon and Washington*. *Weather and Forecasting*, *18*(4), 600–613. https://doi.org/10.1175/1520-0434(2003)018<0600:TIOTMO>2.0.CO;2

Eyring, V., Bony, S., Meehl, G. A., Senior, C. A., Stevens, B., Stouffer, R. J., & Taylor, K. E. (2016). Overview of the Coupled Model Intercomparison Project Phase 6 (CMIP6) experimental design and organization. *Geoscientific Model Development*, *9*(5), 1937–1958. https://doi.org/10.5194/gmd-9-1937-2016

Flato, G., Marotzke, J., Abiodun, B., Braconnot, P., Chou, S. C., Collins, W., et al. (2013). Evaluation of climate models. In: Climate change 2013: The physical science basis. In T. F. Stocker et al. (Eds.), *Contribution of working group I to the fifth assessment report of the intergovernmental panel on climate change* (pp. 741–866). Cambridge, UK and New York, NY: Cambridge University Press.

Fuchs, Ž., & Raymond, D. J. (2017). A simple model of intraseasonal oscillations. *Journal of Advances in Modeling Earth Systems*, *9*, 1195–1211. https://doi.org/10.1002/2017MS000963

Gleckler, P., Doutriaux, C., Durack, P. J., Taylor, K. E., Zhang, Y., Williams, D. N., et al. (2016). A more powerful reality test for climate models. *Eos*, *97*. https://doi.org/10.1029/2016EO051663

Gleckler, P. J., Taylor, K. E., & Doutriaux, C. (2008). Performance metrics for climate models. *Journal of Geophysical Research*, *113*, L06711. https://doi.org/10.1029/2007JD008972

Gonzalez, A. O., & Jiang, X. (2017). Winter mean lower tropospheric moisture over the Maritime Continent as a climate model diagnostic metric for the propagation of the Madden-Julian oscillation. *Geophysical Research Letters*, *44*, 2588–2596. https://doi.org/10.1002/2016GL072430

Hendon, H. H., Wheeler, M. C., & Zhang, C. (2007). Seasonal dependence of the MJO–ENSO relationship. *Journal of Climate*, *20*(3), 531–543. https://doi.org/10.1175/JCLI4003.1

Hersbach, H., Bell, B., Berrisford, P., Horányi, A., Sabater, J. M., Nicolas, J., et al. (2019). Global reanalysis: Goodbye ERA-Interim, hello ERA5. *ECMWF Newsletter*, *159*, 17–24. https://doi.org/10.21957/vf291hehd7

Huffman, G. J., Bolvin, D. T., Nelkin, E. J., Wolff, D. B., Adler, R. F., Gu, G., et al. (2007). The TRMM Multisatellite Precipitation Analysis (TMPA): Quasi-global, multiyear, combined-sensor precipitation estimates at fine scales. *Journal of Hydrometeorology*, *8*(1), 38–55. https://doi.org/10.1175/JHM560.1

Hung, M. P., Lin, J. L., Wang, W., Kim, D., Shinoda, T., & Weaver, S. J. (2013). MJO and convectively coupled equatorial waves simulated by CMIP5 climate models. *Journal of Climate*, *26*(17), 6185–6214. https://doi.org/10.1175/JCLI-D-12-00541.1

Jiang, X. (2017). Key processes for the eastward propagation of the Madden-Julian Oscillation based on multimodel simulations. *Journal of Geophysical Research: Atmospheres*, *122*, 755–770. https://doi.org/10.1002/2016JD025955

Jiang, X., Su, H., & Waliser, D. E. (2019). A Damping Effect of the Maritime Continent for the Madden-Julian Oscillation. *Journal of Geophysical Research: Atmospheres*, *124*, 13,693–13,713. https://doi.org/10.1029/2019JD031503

Jiang, X., Waliser, D. E., Xavier, P. K., Petch, J., Klingaman, N. P., Woolnough, S. J., et al. (2015). Vertical structure and physical processes of the Madden-Julian oscillation: Exploring key model physics in climate simulations. *Journal of Geophysical Research: Atmospheres*, *120*, 4718–4748. https://doi.org/10.1002/2014JD022375

Joyce, R. J., Janowiak, J. E., Arkin, P. A., & Xie, P. (2004). CMORPH: A method that produces global precipitation estimates from passive microwave and infrared data at high spatial and temporal resolution. *Journal of Hydrometeorology*, *5*(3), 487–503. https://doi.org/10.1175/1525-7541(2004)005<0487:CAMTPG>2.0.CO;2

Kiladis, G. N., Dias, J., Straub, K. H., Wheeler, M. C., Tulich, S. N., Kikuchi, K., et al. (2014). A comparison of OLR and circulation-based indices for tracking the MJO. *Monthly Weather Review*, *142*(5), 1697–1715. https://doi.org/10.1175/MWR-D-13-00301.1

Kiladis, G. N., Straub, K. H., & Haertel, P. T. (2005). Zonal and vertical structure of the Madden-Julian oscillation. *Journal of the Atmospheric Sciences*, *62*(8), 2790–2809. https://doi.org/10.1175/JAS3520.1

Kim, D., Sperber, K., Stern, W., Waliser, D., Kang, I.-S., Maloney, E., et al. (2009). Application of MJO simulation diagnostics to climate models. *Journal of Climate*, *22*(23), 6413–6436. https://doi.org/10.1175/2009JCLI3063.1

Kim, D., Kim, H., & Lee, M. I. (2017). Why does the MJO detour the Maritime Continent during austral summer? *Geophysical Research Letters*, *44*, 2579–2587. https://doi.org/10.1002/2017GL072643

Kim, D., Kug, J. S., & Sobel, A. H. (2014). Propagating versus nonpropagating Madden-Julian oscillation events. *Journal of Climate*, *27*(1), 111–125. https://doi.org/10.1175/JCLI-D-13-00084.1

Kim, H. M. (2017). The impact of the mean moisture bias on the key physics of MJO propagation in the ECMWF reforecast. *Journal of Geophysical Research: Atmospheres*, *122*, 7772–7784. https://doi.org/10.1002/2017JD027005

Kiranmayi, L., & Maloney, E. D. (2011). Intraseasonal moist static energy budget in reanalysis data. *Journal of Geophysical Research*, *116*, D21117. https://doi.org/10.1029/2011JD016031

Klotzbach, P. J. (2014). The Madden-Julian Oscillation's impacts on worldwide tropical cyclone activity. *Journal of Climate*, *27*(6), 2317–2330. https://doi.org/10.1175/JCLI-D-13-00483.1

Lee, J., Sperber, K. R., Gleckler, P. J., Bonfils, C. J., & Taylor, K. E. (2019). Quantifying the agreement between observed and simulated extratropical modes of interannual variability. *Climate Dynamics*, *52*(7–8), 4057–4089. https://doi.org/10.1007/s00382-018-4355-4

Lin, J. L., Kiladis, G. N., Mapes, B. E., Weickmann, K. M., Sperber, K. R., Lin, W., et al. (2006). Tropical intraseasonal variability in 14 IPCC AR4 climate models. Part I: Convective signals. *Journal of Climate*, *19*(12), 2665–2690. https://doi.org/10.1175/JCLI3735.1

Ling, J., Zhao, Y., & Chen, G. (2019). Barrier effect on MJO propagation by the Maritime Continent in the MJOTF/GASS models. *Journal of Climate*, *32*(17), 5529–5547. https://doi.org/10.1175/JCLI-D-18-0870.1

Madden, R. A., & Julian, P. R. (1971). Detection of a 40–50 day oscillation in the zonal wind in the tropical Pacific. *Journal of the Atmospheric Sciences*, *28*(5), 702–708. https://doi.org/10.1175/1520-0469(1971)028<0702:DOADOI>2.0.CO;2

Madden, R. A., & Julian, P. R. (1972). Description of global-scale circulation cells in the tropics with a 40–50 day period. *Journal of the Atmospheric Sciences*, *29*(6), 1109–1123. https://doi.org/10.1175/1520-0469(1972)029<1109:DOGSCC>2.0.CO;2

MJOWG (2009). MJO simulation diagnostics. *Journal of Climate*, *22*(11), 3006–3030. https://doi.org/10.1175/2008JCLI2731.1

Raymond, D. J., & Fuchs, Z. (2009). Moisture modes and the Madden-Julian oscillation. *Journal of Climate*, *22*(11), 3031–3046. https://doi.org/10.1175/2008JCLI2739.1

Sobel, A., & Maloney, E. (2013). Moisture modes and the eastward propagation of the MJO. *Journal of the Atmospheric Sciences*, *70*(1), 187–192. https://doi.org/10.1175/JAS-D-12-0189.1

Sperber, K. R. (2003). Propagation and the vertical structure of the Madden–Julian oscillation. *Monthly Weather Review*, *131*(12), 3018–3037. https://doi.org/10.1175/1520-0493(2003)131<3018:PATVSO>2.0.CO;2

Sperber, K. R., & Kim, D. (2012). Simplified metrics for the identification of the Madden-Julian oscillation in models. *Atmospheric Science Letters*, *13*(3), 187–193. https://doi.org/10.1002/asl.378

Takahashi, H. G. (2018). A systematic tropospheric dry bias in the tropics in CMIP5 models: Relationship between water vapor and rainfall characteristics. *Journal of the Meteorological Society of Japan Ser. II*, *96*(4), 415–423. https://doi.org/10.2151/jmsj.2018-046

Taylor, K. E., Stouffer, R. J., & Meehl, G. A. (2012). An overview of CMIP5 and the experiment design. *Bulletin of the American Meteorological Society*, *93*(4), 485–498. https://doi.org/10.1175/BAMS-D-11-00094.1

Wheeler, M., & Kiladis, G. N. (1999). Convectively coupled equatorial waves: Analysis of clouds and temperature in the wavenumber–frequency domain. *Journal of the Atmospheric Sciences*, *56*(3), 374–399. https://doi.org/10.1175/1520-0469(1999)056<0374:CCEWAO>2.0.CO;2

Wheeler, M. C., & Hendon, H. H. (2004). An all-season real-time multivariate MJO index: Development of an index for monitoring and prediction. *Monthly Weather Review*, *132*(8), 1917–1932. https://doi.org/10.1175/1520-0493(2004)132<1917:aarmmi>2.0.co;2

Zhang, C. (2013). Madden-Julian Oscillation: Bridging weather and climate. *Bulletin of the American Meteorological Society*, *94*(12), 1849–1870. https://doi.org/10.1175/BAMS-D-12-00026.1

Zhang, C., & Ling, J. (2017). Barrier effect of the Indo-Pacific Maritime Continent on the MJO: Perspectives from tracking MJO precipitation. *Journal of Climate*, *30*(9), 3439–3459. https://doi.org/10.1175/JCLI-D-16-0614.1